

# Complex delay dynamics of high power quantum cascade oscillators

F. Grillot<sup>1,3\*</sup>, T. C. Newell<sup>2</sup>, A. Gavrielides<sup>3</sup>, and M. Carras<sup>4</sup>

<sup>1</sup>*LTCI, Télécom ParisTech, Université Paris-Saclay, 46 rue Barrault, 75013 Paris, France*

<sup>2</sup>*Air Force Research Laboratory Directed Energy Directorate, Albuquerque NM, USA*

<sup>3</sup>*Center for High Technology Materials, University of New-Mexico, 1313 Goddard SE, Albuquerque, NM, USA*

<sup>4</sup>*mirSense, Centre d'intégration NanoInnov, 8 avenue de la Vauve, 91120 Palaiseau, France*

[grillot@telecom-paristech.fr](mailto:grillot@telecom-paristech.fr)

## ABSTRACT

Quantum cascade lasers (QCL) have become the most suitable laser sources from the mid-infrared to the THz range. This work examines the effects of external feedback in different high power mid infrared QCL structures and shows that different conditions of the feedback wave can produce complex dynamics hence stabilization, destabilization into strong mode-competition or undamping nonlinear oscillations. As a dynamical system, reinjection of light back into the cavity also can also provoke apparition of chaotic oscillations, which must be avoided for a stable operation both at mid-infrared and THz wavelengths.

**Keywords:** Quantum cascade lasers, optical feedback, nonlinear dynamics

## 1. INTRODUCTION

Quantum cascade lasers (QCL) are semiconductor lasers based on ultrafast intersubband transitions with picosecond timescale that have become the most suitable laser sources from the mid-infrared to the THz range, due to their compactness, efficiency and high room temperature performances [1]. In particular, high-power QCLs are powerful sources for optical countermeasures, including night vision blinding and missile out steering. However, some drawbacks arise with high power lasers that usually lead to a strong degradation of the beam quality. A straightforward idea is to increase the width of the QCL active region, in order to increase the volume of the gain region. QCLs as broad as 400- $\mu\text{m}$  have been demonstrated, resulting in peak powers as high as 203 W [2]. However, these wide active regions also result in inefficient heat-load dissipation and strong deterioration of the beam profile. A broader cavity will indeed support numerous transverse modes, leading to degraded far-fields. In interband semiconductor broad area lasers, inducing external perturbations such as optical feedback or optical injection is an efficient technique to control the beam quality and dynamical stability, without resorting to integrated solutions [3,4]. Compared to existing technologies, that are complex and costly, beam shaping with optical feedback is a more flexible solution to obtain high-quality mid-infrared sources. For instance, applying optical feedback enhances the beam quality by reducing substantially the filamentation, which is one of the main issues of high-power laser diodes. The latter corresponds to fast spatio-temporal oscillations, which are due to diffraction of light, self-focusing and spatial hole-burning, whose position along the laser cavity fluctuates with time. Optical feedback can be used to counter the filamentation-induced drawbacks, without altering other performance of the laser [5]. Furthermore, the dynamics ruling a broad-area semiconductor laser are complex, originating from the competition between the many transverse modes that coexist in the cavity. Strong instabilities or even chaos may appear in the emitted signal of a free-running broad-area laser diode, which can also be compensated using optical feedback [6]. Prior work has shown that applying optical feedback enables to efficiently tailor its near-field beam profile. The different cavity modes are sequentially excited by shifting the feedback mirror angle. Further control of the near-field profile is demonstrated using spatial filtering [7]. In this paper, we

examine the effects of external optical feedback in different high power mid infrared QCL structures and discover that the incident angle of the feedback wave can produce complex dynamics hence stabilization, destabilization into strong mode-competition or undamping nonlinear oscillations. More particularly, with a feedback above a few percent, the laser beam can be steered in the far-field using the mirror as the control parameter. In a second regime, very strong mode competition takes place while the last regime shows strong evidence of small amplitude external cavity oscillations. The laser is stable near threshold and a bifurcation occurs with increasing power exciting such external cavity oscillations. As a dynamical system, reinjection of external light back into the cavity also can also provoke possible apparition of chaotic oscillations, which must be avoided for a stable operation [6]. The conclusions supported in this paper can stand both for mid-infrared and THz quantum cascade transmitters.

## 2. OPTICAL FEEDBACK EXPERIMENTAL SETUP

Broad area QCLs tend to oscillate on fewer transverse modes than the number, which can be supported by the waveguide. In cases lasing is dominantly if not totally on a single high-order transverse mode, it leads to a well-defined two-lobed far-field radiation pattern [8]. QCLs possess ultrafast time scales owing to the intersubband transition as well as an almost symmetrical gain with Lorentzian shape hence leading to a near zero linewidth enhancement factor in particular for those emitting at THz wavelengths [1,9]. These traits strongly alter their dynamical behavior over the traditionally studied quantum well laser. The external cavity, shown in Figure 1, consists of the BA-QCL (3 mm length, 40- $\mu\text{m}$  stripe width, HR/AR cleaved facets,  $\lambda=4.6\mu\text{m}$  and  $I_{\text{th}}=1.7\text{A}$ ), aspheric collimating lens ( $f=1.87\text{mm}$ ), coated pellicle beam splitter (55/45 ratio) and mirror. Initially the external cavity is long, 24 cm. The laser was driven with 5- $\mu\text{s}$  pulses at a 10 kHz repetition rate. In subsequent experiments, the cavity was rebuilt as a linear cavity with a partially reflecting mirror ( $R = 67\%$ ) to provide the feedback and could be shortened to 9.6 mm. Pulses are 500 ns or 700 ns to minimize heating effects. Diagnostics consist of a thermopile detector used to measure the power for light-current curves, a mercury cadmium telluride (MCT) high-speed detector to capture the time-series of a pulse at a point in the dimension parallel to the emitter stripe, a Spiricon Pyrocam-III IR camera and a Xenics Onca IR camera. Images from the Spiricon or the Xenics are captured to observe the feedback effect and line-scans are extracted from the data to determine the relative intensity across the image (as shown in Figure 3). Once aligned, the critical parameter for the feedback is the rotation of the mirror. This couples the reflected wave into the cavity at various angles and forces the laser to adjust accordingly.

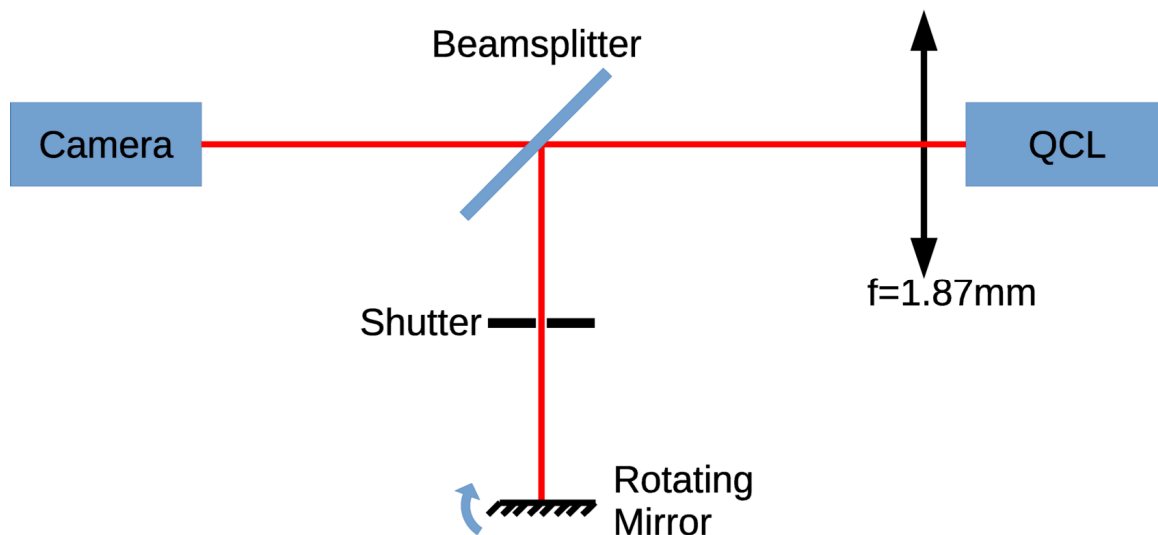


Figure 1. Experimental setup used for the external optical feedback experiments.

The dependency of the near-field depending on the feedback mirror can be understood by considering the rate equations of the BA QCL under optical feedback. The equation governing the complex electric field of the QCL subject to optical feedback is indeed given by [7,10]:

$$\frac{\partial E(x, t)}{\partial t} = \frac{i\pi c^2}{\omega_0 n_{eff}^2} \frac{\partial^2 E(x, t)}{\partial x^2} + \frac{1 + i\alpha}{2} \left( N_{pd} G_0 \Delta N(x, t) - \frac{1}{\tau_p} \right) E(x, t) \quad (1)$$

$$+ kE(x - \Delta x, t - \tau_{ext}) \exp(-i\omega_0 \tau_{ext})$$

where  $c$  is the light velocity,  $\omega_0$  the free-running angular frequency,  $n_{eff}$  the effective refractive index,  $\tau_p$  the photon lifetime inside the laser cavity.  $G_0$  corresponds to the net modal gain for one period,  $N_{pd}$  to the number of periods,  $\alpha$  to the linewidth enhancement factor and  $\tau_{ext}$  to the external cavity roundtrip time.  $N$  is the carrier density difference between the upper and the lower lasing states. Finally,  $k$  is the feedback coefficient, defined in the case of Fabry-Perot lasers as:

$$k = \frac{1}{\tau_{in}} \frac{1 - R_2}{\sqrt{R_2}} \sqrt{f_{ext}} \quad (2)$$

with  $\tau_{in}$  the internal cavity roundtrip time,  $R_2$  the front facet reflectivity (here  $R_2=0.3$ ) and  $\sqrt{f_{ext}}=r_3$  the feedback ratio, i.e. the ratio between reinjected and emitted light with  $r_3$  the reflection coefficient of the feedback mirror. In BA lasers, the dependency of the field and carrier densities on the spatial variable  $x$  becomes very important, as underlined by the diffraction term in the complex field rate equation. A diffusion term  $D_n$  furthermore exists in the carrier rate equation, and for an interband laser under optical feedback, it can be written as [7,10]:

$$\frac{\partial N(x, t)}{\partial t} = D_n \frac{\partial^2 N(x, t)}{\partial x^2} + \frac{I}{q} - \frac{N(x, t)}{\tau_c} - G(N(x, t))|E|^2 \quad (3)$$

In a QCL, several diffusion coefficients corresponding to the several carrier rate equations have to be considered. Moreover, when applying optical feedback, the reinjected mode is not necessarily superimposed on the corresponding emitted mode, it can be shifted by a quantity  $\Delta x$ . It will therefore be crucial to control precisely the angle of the mirror when applying optical feedback to BA QCLs. To this end, it is important to note that the mirror rotation angle also alters the fraction of light coupled into the waveguide. For the 24 cm external cavity, the maximum laser threshold reduction,  $\Delta I/I$ , was  $\sim 7\%$ . For shorter cavities the threshold reduction was as high as 15%.

### 3. EXPERIMENTAL RESULTS

Figure 2(a) shows the light-voltage-current curves for a typical 40- $\mu\text{m}$  stripe BA QCL. With 500 ns pulses and 0.5% duty cycle, over 5W peak power can be developed at a current just over 3A, which is one motivation for investigating BA-QCLs. Figure 2(b) is a line scan of the intensity extracted from a near field image of the facet for the free running case. In the far field, this evolves into a dual lobe pattern. It is quite remarkable that BA-QCLs predominantly lase on a single high-order transverse mode, see for example Ref. [4]. While this particular laser shows other transverse modes, its primary mode is  $M=9$ . Optical spectra of the laser show that a number of longitudinal laser lines are oscillating. As shown in Figure 3, when varying the angle of the feedback mirror, the shape of the QCL near-field is significantly impacted by optical feedback. In each configuration, the profile is calculated by summing the intensities on each pixel column, and the inset

presents directly the near-field recorded on the camera. Compared to the free-running case, an intensity peak can appear either centered or off-centered on the beam profile, or the near-field can be completely evened.

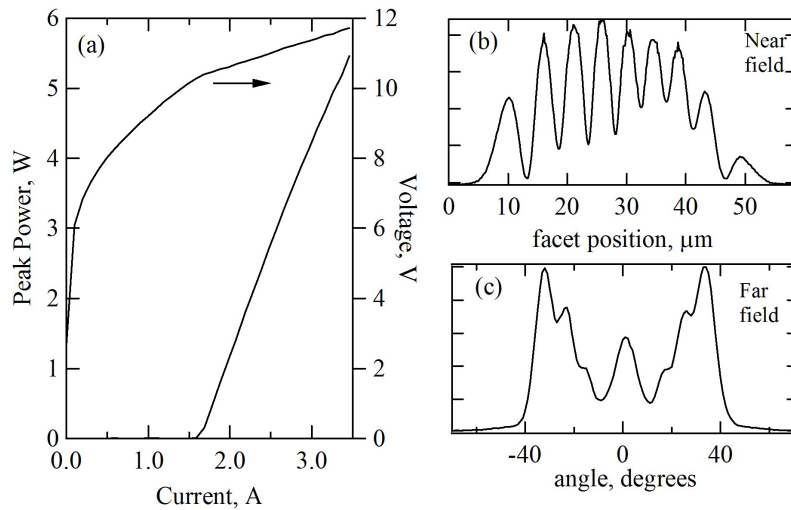


Figure 2. Free running laser characteristics of the BA QCL. (a) Power voltage curve. (b) Intensity line scan at the facet measured at 1.82 A. (c) Beam divergence angles.

In one case, feedback can be selected to improve the brightness of the laser. Figure 4 shows the light current curves of the free-running and feedback case. (Note that the power is now measured after the feedback mirror and is less than the total power of the laser.) The threshold reduction is 13%. The near field image, Fig. 4(b), shows that most of the power is in a single spot, which is in the same location as an antinode of the M=9 mode. At a distance of 2.4 mm from the cavity the MCT detector (1-ns rise-time) is translated across the beam front. Figure 4(c) shows a single strong peak indicating that the laser brightness can be strongly improved over the free running case.

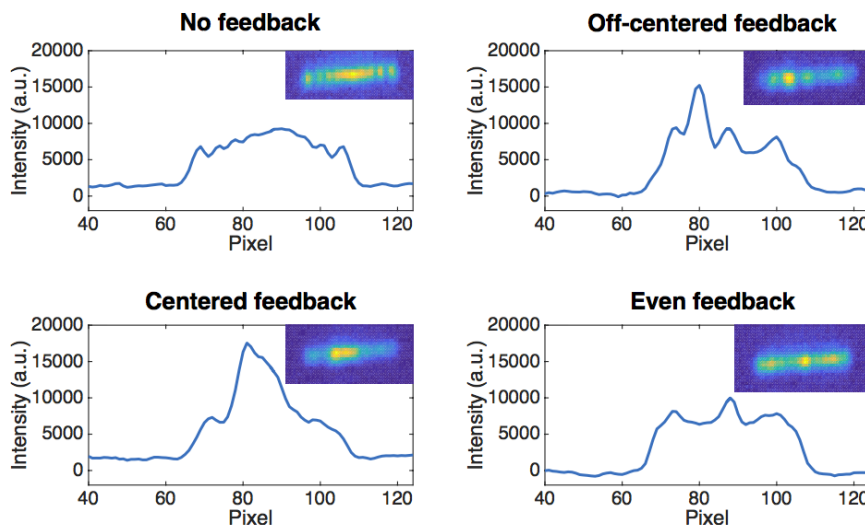


Figure 3. Near-field at the laser facet for several feedback angle. Plots in inset correspond to the near-field image recorded on the camera.

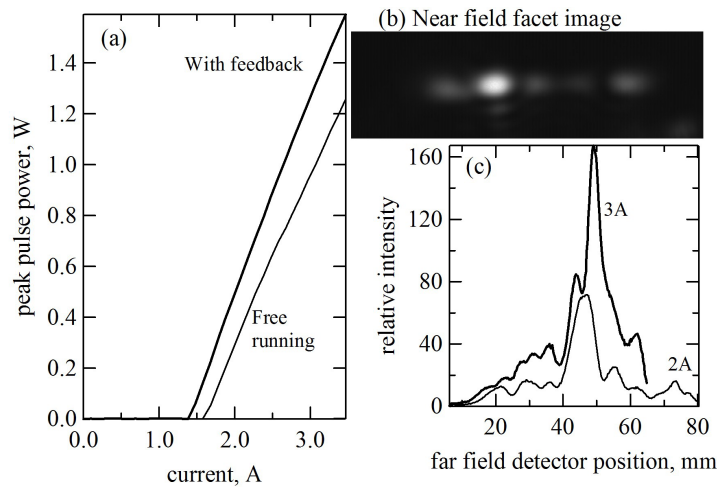


Figure 4. High brightness case. (a) The threshold is reduced 13% and power increased over the free running case, (b) an image of the facet. (c) The far field shows a single peak and improved brightness over the free running beam.

The temporal response of the laser pulse is also observed with the high-speed MCT detector, and the observations point to three principal regimes of dynamics. The first is a regime of stability that is characterized by a pulse shape similar to the free-running case although different in amplitude. Significantly, very small amounts of feedback,  $\Delta I/I < 1\%$ , are sufficient to alter the modal intensity. No high frequency oscillations or large amounts of noise are observed. With feedback above a few percent, the laser beam can be effectively *steered in the far-field using the mirror as the control parameter*. In a second regime, mode competition occurs in addition to the altering the far field beam profile. In the long 24-cm cavity highly erratic strong power drop-outs were observed that may be impacted by several external cavity modes (ECM) hence leading to more complex dynamics between ECMs and cavity ones. In the shorter cavities for which the number of ECM is strongly reduced, more regular mode beating occurs. Figure 5 shows one particular case where the mode competition exhibits regular oscillations. Two time series are shown with the second shifted vertically for ease of view. The lower time series is at a point in the beam while the upper time series is taken at a different location, 4mm away. It shows mode beating with power regularly switching back and forth. Regardless of the mirror rotation angle, when such oscillations are observed; the time scales are in the 10 s of nanoseconds ( $T \sim 56$  ns in Fig. 5) and their frequency increases as the current increases.

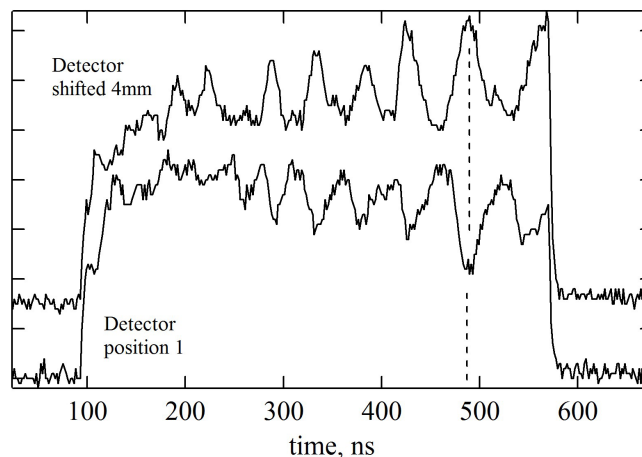


Figure 5. Pulse time series taken at two points in the far field of the beam. The power in the transverse modes oscillates at  $\sim 18$  MHz but is current dependent.

The last (third) regime shows strong evidence of small amplitude external cavity oscillations that arise from the round-trip time delay of the feedback. The time-series, Fig. 6(a), show a very distinct signature. Time series for 700ns pulses are shown near threshold and up to 2.05A. The laser is stable near threshold and a bifurcation occurs with increasing power exciting these external cavity oscillations. Fig 6(b) is a zoom in of the time series taken at 1.6A over a 100ns range. Fast-Fourier transforms of the pulses shows oscillations in the 300 MHz to 500 MHz range with the frequency increasing with current. In addition, chaotic dynamic driven by low frequency fluctuations from the mode competition also can be observed.

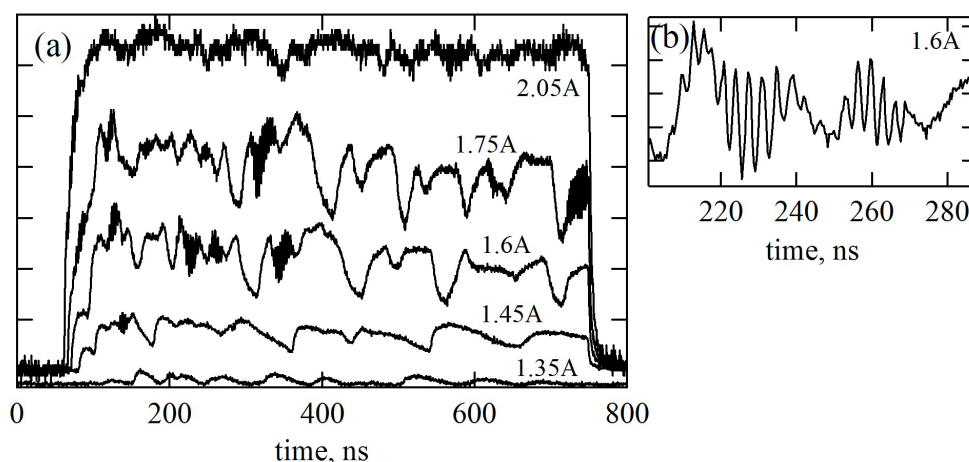


Figure 6. Time series at 1.35A, 1.45A, 1.6A, 1.75A and 2.05A. (b) a close up of the 1.6A time series. The fast oscillations are almost certainly related to a bifurcation process. Digitization aliasing is most likely occurring since the external cavity round trip time is too fast for our setup.

It is critical to point out that the detector has a rise-time of only 1ns and is digitized by the oscilloscope at 800-ps intervals to reflect this limited bandwidth. Thus the oscillations are almost certainly an aliasing effect of the digitization process. For this particular arrangement, the external cavity round trip time should show fluctuations near 4.8 GHz. Nevertheless, these traces are almost certainly evidence that external cavity oscillations are occurring. At 2.05A the time series is very noisy. It is unclear whether very high frequency oscillations are being recorded or it is simply detector and amplifier noise. The measurements are fundamentally limited by the detector responsivity and its associated amplifier. It would be necessary to repeat these measurements with higher resolution equipment, to conclude on whether these oscillations occur at the external cavity frequency, as in the case of narrow-ridge QCLs. Compared to the free-running scenario, an increase or decrease of the power may appear, either on the totality or on only part of the temporal peak power during the pulse. We do not have a direct link of these temporal responses with a specific mirror position but can say that whereas coupling light into the cavity is quite easy, finding conditions to trigger these oscillations requires some effort. Alignment is critical. The BA-QCL is very stable in this aspect.

A summary of our observations is as follows. The free running BA-QCL predominantly lases on a single high order transverse mode along with multiple longitudinal modes. Small amounts of feedback are easily sufficient to modify emission but appear to do so by modifying the amplitude of the electric field at each antinode of the principal mode, without changing the mode number. And the effect is to readily steer the beam in the far field. With a judicious choice of mirror angle the BA-QCL exhibits both high power operation and a single far field intensity peak, which is very interesting for various pointing applications. At higher levels of feedback, mode competition usually occurs with pump dependent time scales ranging from 15 ns to 80 ns. Under certain conditions very high frequency, ~500 MHz, oscillations are observed. The observed oscillations are probably a digitization aliasing recreation of the much faster external cavity round-trip

oscillations. The driver for this nonlinear effect is the pump current. However, the role of the cavity dimensions, any intracavity components, mirror angle and feedback strength remains unknown.

## CONCLUSIONS

These initial results provide some clues to help anchor modeling efforts and directs future experimental work. Some guidelines have been found regarding back reflections of light from optical components such as collimating optics or mirrors. Beyond self-feedback further work will also investigate the coupling of linear arrays of emitters in the so-called Talbot configuration for phase-locking operation using broad area emitters [11]. The results are of paramount importance for creating a bright infrared source with Watt-level power.

## ACKNOWLEDGMENTS

The authors acknowledge the financial support of the U.S. Air Force Office of Scientific Research.

## REFERENCES

- [1] Faist, J., Quantum Cascade Lasers, Oxford University Press (2013).
- [2] Heydari, D., Bai, Y., Bandyopadhyay, N., Slivken, S., and Razeghi, M., "High brightness angled cavity quantum cascade lasers," *Appl. Phys. Lett.* 106(9), 091105 (2015).
- [3] Marciante, J. R. and Agrawal, G. P., "Lateral spatial effects of feedback in gain-guided and broad-area semiconductor lasers," *IEEE J. Quantum Electron.* 32(9), 1630–1635 (1996).
- [4] Mandre, S. K., Fischer, I., and Elsaesser, W., "Spatiotemporal emission dynamics of a broad-area semiconductor laser in an external cavity: Stabilization and feedback-induced instabilities," *Opt. Commun.* 244, 355–365 (2005).
- [5] Tachikawa, T., Takimoto, S., Shogenji, R., and Ohtsubo, J., "Dynamics of broad-area semiconductor lasers with short optical feedback," *IEEE J. Quantum Electron.* 46(2), 140–149 (2010).
- [6] Jumpertz, L., Schires, K., Carras, M., Sciamanna, M., and Grillot, F., "Chaotic light at mid-infrared wavelength," *Nature Light Sci. Appl.* 5, e16088 (2016).
- [7] Ferré, S., Jumpertz, L., Carras, M., Ferreira, R., and Grillot, F. "Beam shaping in high-power broad-area quantum cascade lasers using optical feedback," *Nature Scientific Reports*, 7:44284, (2017).
- [8] Bai, Y., Slivken, S., Darvish, S.R., Haddadi A., Gokden B. and Razeghi, M., "High power broad area quantum cascade lasers," *Appl. Phys. Lett.* 95, 221104 (2009).
- [9] Jumpertz, L., Michel, F., Pawlus, R., Elsaesser, W., Schires, K., Carras, M., and Grillot, F., "Measurements of the linewidth enhancement factor of mid-infrared quantum cascade lasers by different optical feedback techniques," *AIP Advances*, 6, 015212, (2016).
- [10] Takeda, A., Shogenji, R., and Ohtsubo, J., "Spatial-mode analysis in broad-area semiconductor lasers subjected to optical feedback," *Opt. Rev.*, 20(4), 308, (2013).
- [11] Wang, L., Zhang, J., Jia, Z., Zhao, Y., Liu, C., Liu, Y., Zhqi S., Ning, Z., Xu, X., and Liu, F., "Phase-locked array of quantum cascade lasers with an integrated Talbot cavity," *Optics Express*, 24(26), 30275-30281, (2016).